

# Alignment and integration of complex networks by hypergraph-based spectral clustering

Tom Michoel\*

*Freiburg Institute for Advanced Studies (FRIAS), University of Freiburg,  
Albertstrasse 19, D-79104 Freiburg, Germany and  
The Roslin Institute, The University of Edinburgh,  
Easter Bush, Midlothian, EH25 9RG, Scotland, UK*

Bruno Nachtergaele†

*Department of Mathematics, University of California Davis,  
One Shields Avenue, Davis, CA 95616-8366, USA*

Complex networks possess a rich, multi-scale structure reflecting the dynamical and functional organization of the systems they model. Often there is a need to analyze multiple networks simultaneously, to model a system by more than one type of interaction or to go beyond simple pairwise interactions, but currently there is a lack of theoretical and computational methods to address such problems. Here we introduce a framework for multi-network analysis based on hypergraph representations. Our main result is a generalization of the Perron-Frobenius theorem from which we derive spectral clustering algorithms for directed and undirected hypergraphs. We illustrate our approach with applications for tripartite community detection in folksonomies, for local and global alignment of protein-protein interaction networks between multiple species and for detecting clusters of overlapping regulatory pathways in directed networks.

## I. INTRODUCTION

Complex networks in nature and society represent pairwise interactions between entities in inhomogeneous systems and understanding their structure and function has been the focus of much research. At the macroscopic scale, complex networks are characterized by, among others, a degree distribution, characteristic path length and clustering coefficient which are markedly different from those of regular lattices or uniformly distributed Erdős-Rényi random graphs [1, 2], while at the microscopic scale, they contain network motifs, small subgraphs occurring significantly more often than expected by chance [3]. The intermediate level usually exhibits the presence of communities or modules, sets of nodes with a significantly higher than expected density of links between them, typical examples being friendship circles in social networks, websites devoted to similar topics in the World Wide Web or protein complexes in protein interaction networks [4].

However, the limitations of modeling a complex system by a network with a single type of pairwise interaction are becoming more and more clear. Folksonomies, online social communities where users apply tags to annotate resources such as images or scientific articles, have a tripartite structure with three types of interactions [5, 6]. In biology, cellular systems are characterized by different types of networks which represent different physical interaction mechanisms operating on different time-scales, intertwined with each other through extensive feedforward

and feedback loops [7, 8]. To understand how evolutionary dynamics shapes molecular interaction networks, we need to compare them between multiple species with non-trivial many-to-many relations between their respective node sets [9]. In order to move beyond simple networks of pairwise interactions to model these and other systems, one suggestion has been to use hypergraphs, where edges are arbitrarily sized subsets of nodes. Although a number of studies have generalized various concepts from graph theory to hypergraphs [5, 6, 10–13], a rigorous mathematical foundation and general-purpose algorithm for clustering and community detection in hypergraphs, which addresses concrete problems in multi-network analysis, is still lacking. Here we present a framework for spectral clustering in hypergraphs which is mathematically sound and algorithmically efficient. We demonstrate its use through several practical applications in the analysis of large-scale, real-world networks.

## II. GRAPHS AND HYPERGRAPHS

A graph  $\mathcal{G}$  is defined as a pair  $(\mathcal{V}, \mathcal{E})$  of vertices  $\mathcal{V}$  and edges (pairs of vertices)  $\mathcal{E}$ , which may be directed or not. In a weighted graph, a number is assigned to each edge which may represent, *e.g.*, the cost, length or reliability of an edge. A hypergraph is a generalization of a graph where an edge, called hyperedge in this case, can connect any number of vertices, *i.e.*,  $\mathcal{E}$  is a set of arbitrarily sized subsets of  $\mathcal{V}$ . A particular class of hypergraphs are so-called  $k$ -uniform hypergraphs where each hyperedge has the same cardinality  $k$ . Algebraically, a graph can be represented by an adjacency matrix  $A$  of dimension  $N \times N$ , with  $N$  the number of vertices, such that  $A_{ij} = 1$  if  $\{i, j\} \in \mathcal{E}$  and 0 otherwise. For undi-

---

\* tom.michoel@roslin.ed.ac.uk

† bxn@math.ucdavis.edu

rected graphs,  $A$  is a symmetric matrix and for weighted graphs,  $A_{ij}$  is defined to be the weight of the edge  $\{i, j\}$ . For  $k$ -uniform hypergraphs, the notion of adjacency matrix can be generalized to an adjacency multi-array or tensor  $T$  such that  $T_{i_1 \dots i_k} = 1$  if  $\{i_1, \dots, i_k\} \in \mathcal{E}$  and 0 otherwise. For a general hypergraph, we define a function  $w$  on the set of subsets of  $\mathcal{V}$  such that  $w(E) = 1$  for  $E \in \mathcal{E}$  and 0 otherwise. In general, we allow weighted hypergraphs where  $w$  can be any nonnegative function. We say a hypergraph is reducible if there exists a proper vertex subset  $I \subset \mathcal{V}$  such that for any  $i \in I$  and any  $j_1, \dots, j_m \notin I$ ,  $w(\{i, j_1, \dots, j_m\}) = 0$ , and irreducible if it is not reducible. Directed hypergraphs can be defined in many ways. For instance for  $k$ -uniform hypergraphs, we can impose any form of permutation symmetry, or lack thereof, between some or all of the  $k$  dimensions in each edge. In this paper, we will only consider the case where each edge  $E$  can be written as a pair  $(S, T)$ , where  $S \subset \mathcal{V}$  is called the ‘source’ vertex set and  $T \subset \mathcal{V}$  the ‘target’ vertex set, with weight function  $w(S, T)$ . The inverse of such a directed hypergraph is defined by the weight function  $w'(S, T) = w(T, S)$ . A directed hypergraph is reducible if there exists a proper vertex subset  $I \subset \mathcal{V}$  such that for any  $i \in I$  and any  $j_1, \dots, j_m, k_1, \dots, k_n \notin I$ ,  $w(\{i, j_1, \dots, j_m\}, \{k_1, \dots, k_n\}) = 0$ , and irreducible if neither the hypergraph nor its inverse are reducible.

### III. DOMINANT EIGENVECTORS AND SPECTRAL GRAPH CLUSTERING

Although countless measures have been designed to define clusters in a graph [14, 15], perhaps the simplest definition is that a cluster is a subset of vertices with a high number of edges between them, relative to its size. Mathematically, for a graph with adjacency matrix  $A$ , the edge-to-node ratio of a subset  $X \subset \mathcal{V}$  can be written as

$$\mathcal{S}(X) = \frac{\sum_{i,j \in X} A_{ij}}{|X|},$$

where  $|X|$  denotes the number of elements in  $X$ . The number of subsets of a set with  $N$  elements grows exponentially in  $N$  and hence finding the subset with maximal edge-to-node ratio by exhaustive enumeration is computationally infeasible for large graphs. However, if we denote by  $u_X$  the unit vector in  $\mathbb{R}^N$  which has  $u_{X,i} = |X|^{-1/2}$  for  $i \in X$  and 0 otherwise, we can write  $\mathcal{S}$  as a scalar product and obtain the simple upper bound:

$$\mathcal{S}(X) = \langle u_X, Au_X \rangle \leq \max_{x \in \mathbb{R}^N, x \neq 0} \frac{\langle x, Ax \rangle}{\|x\|^2} = \lambda_{\max}, \quad (1)$$

where  $\langle x, y \rangle = \sum_i x_i y_i$  is the standard inner product on  $\mathbb{R}^N$ ,  $\|x\| = \sqrt{\langle x, x \rangle}$  is the length of  $x$ , and  $\lambda_{\max}$  is the largest eigenvalue of  $A$ . By the Perron-Frobenius theorem [16], if the graph is irreducible, the dominant eigenvector  $x$ , which satisfies  $\lambda_{\max} x = Ax$ , is unique, strictly

positive ( $x_i > 0$  for all  $i$ ), and solves the variational problem in the r.h.s. of eq. (1).

Hence, to find an approximate maximizer  $X$  of  $\mathcal{S}$ , we can take the set  $X$  for which  $u_X$  is as close as possible to the dominant eigenvector  $x$ , similar to what is done in other spectral clustering algorithms based on the Laplacian or modularity matrices [17], *i.e.*, define

$$\tilde{X} = \operatorname{argmax}_{X \subset \mathcal{V}} \langle u_X, x \rangle = \operatorname{argmax}_{X \subset \mathcal{V}} \frac{1}{|X|^{1/2}} \sum_{i \in X} x_i.$$

Since  $x > 0$ ,  $\tilde{X}$  is of the form  $X_c = \{i: x_i > c\}$  for some threshold value  $c$ . Instead of  $\tilde{X}$ , we therefore choose as an approximate maximizer the solution of the restricted variational problem

$$X_{\max} = \operatorname{argmax}_{c > 0} \mathcal{S}(X_c). \quad (2)$$

Solving eq. (2) is linear in the number of vertices, since we only need to consider the values  $c$  equal to the entries of  $x$ . Moreover,  $\mathcal{S}(X_{\max}) \geq \mathcal{S}(\tilde{X})$ , and hence  $X_{\max}$  is a better approximation to the true maximizer of  $\mathcal{S}$  than  $\tilde{X}$ .

Thus we obtain a numerically highly efficient spectral graph clustering algorithm:

1. Calculate the dominant eigenvector  $x$  using for instance a power method [18].
2. Find the cluster  $X_{\max}$  which solves the restricted variational problem in eq. (2).
3. Store  $X_{\max}$ , remove all edges between nodes in  $X_{\max}$  from the edge set  $\mathcal{E}$ , and repeat the procedure until no more edges remain.

This algorithm is an edge clustering algorithm and finds potentially overlapping clusters. Alternatively, in step 3 we can remove all vertices in  $X_{\max}$  to generate non-overlapping clusters.

This procedure generalizes immediately to directed graphs. In this case a cluster consists of a ‘source’ set  $X$  and ‘target’ set  $Y$  with edge-to-node ratio

$$\mathcal{S}(X, Y) = \frac{\sum_{i \in X, j \in Y} A_{ij}}{\sqrt{|X| \cdot |Y|}}.$$

The dominant eigenvector is replaced by the dominant left and right singular vectors  $x$  and  $y$  corresponding to the largest singular value of  $A$ , which are again unique and strictly positive [16].  $X_{\max}$  and  $Y_{\max}$  are found by maximizing  $\mathcal{S}(X, Y)$  over sets obtained by thresholding on the entries of  $x$  and  $y$ .

### IV. PERRON-FROBENIUS THEOREM FOR HYPERGRAPHS

Our aim is to generalize the previous graph spectral clustering algorithm to arbitrary hypergraphs. For this

purpose we first need a generalization of the Perron-Frobenius theorem. Let  $\mathcal{H} = (\mathcal{V}, \mathcal{E})$  be an undirected hypergraph on  $N$  vertices. Define for  $x \in \mathbb{R}^N$  and  $p \geq 1$

$$\mathcal{R}_p(x) = \sum_{E \in \mathcal{E}} w(E) \prod_{i \in E} \left( \frac{|x_i|}{\|x\|_p} \right)^{\frac{1}{|E|}}, \quad (3)$$

where  $w(E)$  is the nonnegative weight of edge  $E$  and  $\|x\|_p = (\sum_i |x_i|^p)^{1/p}$  is the  $p$ -norm of  $x$ . We have the following key result:

**Theorem 1.**  $\mathcal{R}_p$  attains its maximum on the set of unit vectors  $\mathbb{S}_p^N = \{u \in \mathbb{R}^N : \|u\|_p = 1\}$ . If  $\mathcal{H}$  is irreducible, there is a unique maximizer  $x \in \mathbb{S}_p^N$  which is strictly positive and satisfies the Euler-Lagrange equations

$$\lambda_p x_i^p = \sum_{E \ni i} \frac{w(E)}{|E|} \left( \prod_{j \in E} x_j \right)^{\frac{1}{|E|}}, \quad (4)$$

subject to the constraint  $\|x\|_p = 1$  and with  $\lambda_p = \mathcal{R}_p(x)$ . By analogy with the matrix case, we call  $x$  the dominant eigenvector of  $\mathcal{H}$ .

*Proof.* Existence of a maximizer on  $\mathbb{S}_p^N$  follows from Weierstrass's theorem [16]. Clearly, since  $\mathcal{R}_p(x) = \mathcal{R}_p(|x|)$ , we can always choose a maximizer  $x$  to have nonnegative entries. Hence we can find  $x$  as a stationary point of the Lagrangian

$$\mathcal{L}(x) = \sum_{E \in \mathcal{E}} w(E) \left( \prod_{i \in E} |x_i| \right)^{\frac{1}{|E|}} - \frac{\lambda}{p} (\|x\|_p^p - 1),$$

giving rise (for nonnegative  $x$ ) to the Euler-Lagrange equations

$$\lambda x_i^{p-1} = \sum_{E \ni i} \frac{w(E)}{|E|} \left( \prod_{j \in E, j \neq i} x_j \right)^{\frac{1}{|E|}} x_i^{\frac{1}{|E|} - 1}. \quad (5)$$

Let  $I = \{i \in \mathcal{V} : x_i = 0\}$  and  $i \in I$ . Assume there exists an edge  $E = \{i, j_1, \dots, j_m\}$  with  $j_1, \dots, j_m \notin I$ . Then the l.h.s. of eq. (5) is 0 while the r.h.s. is  $\infty$ . Hence such an edge cannot exist, but this contradicts the assumption of irreducibility of  $\mathcal{H}$ . It follows that  $I = \emptyset$  or  $x > 0$ . For  $x > 0$  we can multiply both sides of eq. (5) by  $x_i$  and obtain eq. (4). Summing both sides in eq. (4) over  $i$  gives  $\lambda_p = \mathcal{R}_p(x) = \max_{x'} \mathcal{R}_p(x')$ .

Next assume  $y > 0$  is another maximizer of  $\mathcal{R}_p$ . Denote  $c = \min_i (x_i/y_i)$ ,  $u = cy$ , and  $z = x - u \geq 0$ . Since  $\|x\|_p = \|y\|_p = 1$ , we have  $c < 1$  and  $c^p \leq c$  for  $p \geq 1$ . Denote  $I = \{i \in \mathcal{V} : z_i = 0\}$ . For any  $i \in I$ , by the Euler-Lagrange equations,

$$0 = \lambda_p (x_i^p - c^p y_i^p) \geq \sum_{E \ni i} w(E) \left[ \left( \prod_{j \in E} x_j \right)^{\frac{1}{|E|}} - \left( \prod_{j \in E} u_j \right)^{\frac{1}{|E|}} \right].$$

Since each term in the last sum is positive, they must all be zero. Hence for any  $j_1, \dots, j_k \notin I$ , if  $\{i, j_1, \dots, j_k\} \in \mathcal{E}$

then

$$\begin{aligned} 0 &= \prod_{m=1}^k x_{j_m} - \prod_{m=1}^k u_{j_m} \\ &= \sum_{m=1}^k \left( \prod_{n=1}^{m-1} u_{j_n} \right) (x_{j_m} - u_{j_m}) \left( \prod_{n=m+1}^k x_{j_n} \right). \end{aligned}$$

Again each term in this sum is positive and must therefore be zero, but this contradicts  $j_1, \dots, j_k \notin I$ . Hence edges with  $i \in I$  and  $j_1, \dots, j_k \notin I$  do not exist, but this contradicts the assumption of irreducibility. Since  $I \neq \emptyset$ , we must have  $I = \mathcal{V}$  or  $x = y$ .  $\square$

Next consider directed hypergraphs with hyperedges  $E = (S, T)$ ,  $S, T \subset \mathcal{V}$  as defined before. Then define  $\mathcal{R}_{p,q}(x, y)$  for  $x, y \in \mathbb{R}^N$  and  $p, q \geq 1$

$$\mathcal{R}_{p,q}(x, y) = \sum_{S, T \subset \mathcal{V}} w(S, T) \prod_{i \in S} \left( \frac{|x_i|}{\|x\|_p} \right)^{\frac{1}{2|S|}} \prod_{j \in T} \left( \frac{|y_j|}{\|y\|_q} \right)^{\frac{1}{2|T|}}.$$

By identical arguments as before, it can be shown that for an irreducible hypergraph, there exists a unique pair  $x \in \mathbb{S}_p^N$  and  $y \in \mathbb{S}_q^N$  such that  $\mathcal{R}_{p,q}(x, y) \geq \mathcal{R}_{p,q}(x', y')$  for all  $x', y' \in \mathbb{R}^N$ . These maximizers are strictly positive and satisfy the Euler-Lagrange equations

$$\lambda_{p,q} x_i^p = \sum_{S \ni i, T} \frac{w(S, T)}{|S|} \left( \prod_{i \in S} x_i \right)^{\frac{1}{2|S|}} \left( \prod_{j \in T} y_j \right)^{\frac{1}{2|T|}} \quad (6)$$

$$\lambda_{p,q} y_i^q = \sum_{S, T \ni i} \frac{w(S, T)}{|T|} \left( \prod_{i \in S} x_i \right)^{\frac{1}{2|S|}} \left( \prod_{j \in T} y_j \right)^{\frac{1}{2|T|}}, \quad (7)$$

subject to the constraints  $\|x\|_p = \|y\|_q = 1$  and with  $\lambda_{p,q} = \mathcal{R}_{p,q}(x, y)$ .

## V. SPECTRAL CLUSTERING AND BICLUSTERING IN HYPERGRAPHS

Having a generalization of the Perron-Frobenius theorem, it is straightforward to also generalize the spectral clustering method. Define for  $X \subset \mathcal{V}$ ,

$$\mathcal{S}_p(X) = \frac{\sum_{E \subset X} w(E)}{|X|^{\frac{1}{p}}} = \mathcal{R}_p(u_X) \leq \mathcal{R}_p(x),$$

with  $x$  the dominant eigenvector and  $u_X \in \mathbb{S}_p^N$  now defined by  $u_{X,i} = |X|^{-1/p}$  for  $i \in X$  and 0 otherwise. The parameter  $p$  balances cluster size versus edge density. For  $p = 1$ ,  $\mathcal{S}_p$  is simply the ratio of edges to nodes in  $X$ . Taking  $p > 1$  diminishes the influence of the denominator and progressively favors to have a high number of edges rather than a high number of edges per node in high-scoring clusters. The spectral clustering algorithm becomes:

1. Calculate the maximizer  $x$  of  $\mathcal{R}_p$ .

- Find the cluster  $X_{\max}$  which solves the restricted variational problem

$$X_{\max} = \operatorname{argmax}_{c>0} \mathcal{S}_p(X_c)$$

with  $X_c = \{i \in \mathcal{V}: x_i > c\}$ .

- Store  $X_{\max}$ , remove all hyperedges between nodes in  $X_{\max}$  from the edge set  $\mathcal{E}$ , and repeat the procedure until no more hyperedges remain.

The maximizer can be calculated using a generalization of the power method for matrices [18] or tensors [19]: starting with an initial vector  $x^{(0)}$ , we compute  $x^{(n+1)}$  from  $x^{(n)}$  using the Euler-Lagrange equations (4)

$$x_i^{(n+1)} \leftarrow \left[ \sum_{E \ni i} \frac{w(E)}{|E|} \left( \prod_{j \in E} x_j^{(n)} \right)^{\frac{1}{|E|}} \right]^{\frac{1}{p}}$$

$$x_i^{(n+1)} \leftarrow \frac{x_i^{(n+1)}}{\|x^{(n+1)}\|_p},$$

iterated until some stationarity criterion on the components of  $x^{(n)}$  is met. Due to the uniqueness of  $x$ , the choice of starting vector is not important. By taking a nonnegative one, such as the uniform vector  $x^{(0)} = [1, 1, \dots, 1]^T / N^{1/p}$ , we ensure that the powers of  $1/|E|$  occurring in the Euler-Lagrange equations are always defined unambiguously. Many of the hypergraphs occurring in real-world applications are not irreducible. In such cases it is important to ensure that  $x^{(0)}$  has support only on a single irreducible component to obtain the unique maximizer for that component.

Although we typically view a cluster as a subset of vertices, it is actually a subset of hyperedges (all hyperedges  $E \subset X_{\max}$ ) and thus can be considered as a sub-hypergraph as well. We found that, especially for large networks with thousands of hyperedges, higher scores are usually obtained by recursively applying the previous procedure to each of the clusters itself.

For directed hypergraphs, we obtain a biclustering method. Define for  $X, Y \subset \mathcal{V}$  and  $p, q \geq 1$

$$\mathcal{S}_{p,q}(X, Y) = \frac{\sum_{S \subset X, T \subset Y} w(S, T)}{|X|^{\frac{1}{2p}} |Y|^{\frac{1}{2q}}}.$$

Approximate maximizers  $X_{\max}$  and  $Y_{\max}$  are found by solving the restricted variational principle

$$(X_{\max}, Y_{\max}) = \operatorname{argmax}_{(c_1, c_2)} \mathcal{S}_{p,q}(X_{c_1}, Y_{c_2}),$$

with  $X_c = \{i \in \mathcal{V}: x_i > c\}$  and  $Y_c = \{i \in \mathcal{V}: y_i > c\}$ , where  $x$  and  $y$  are the unique solutions of the Euler-Lagrange equations (6)-(7), which can again be calculated using a power algorithm.

## VI. RELATION TO PREVIOUS WORK

The matrix algorithm for clustering in a simple graph has its roots in a method for image pattern recognition [20] and using the singular value decomposition to detect densely linked sets in directed networks goes back to the work of J. Kleinberg [21]. The novelty here lies in the definition of a discrete cluster through solving the restricted variational problem, instead of using an ad-hoc cut-off on the eigenvector entries. For  $k$ -uniform hypergraphs, we can define rescaled variables  $y_i = x_i^{1/k}$  such that maximizing  $\mathcal{R}_p(x)$  becomes equivalent to maximizing

$$\mathcal{R}'_{p'}(y) = \frac{\sum_{i_1, \dots, i_k} T_{i_1 \dots i_k} y_{i_1} \dots y_{i_k}}{\|y\|_{p'}^k}$$

with  $p' = kp$ . In this case, Theorem 1 reduces to a multilinear extension of the Perron-Frobenius theorem to non-negative irreducible tensors of arbitrary dimension, which has been the subject of several recent papers [22–24]. The proof given in Theorem 1 is however considerably simpler and follows more closely the proof of the matrix theorem [16]. In the unscaled variational problem for  $\mathcal{R}'_{p'}$ , the maximizer is unique for  $p' \geq k$  and thus it is unsuited for generalizing to arbitrary hypergraphs where the uniqueness condition would become  $p' \geq k_{\max}$ , the maximum edge size in the hypergraph. This explains why we introduced the geometric average over the values  $x_j$  in eq. (3). To the best of our knowledge, Theorem 1 is the first proof of a Perron-Frobenius theorem for general hypergraphs.

For  $k = 3$ , we have previously used a similar approach to find clusters of 3-node network motifs in integrated interaction networks [25, 26]. In this case an adjacency tensor  $T_{rst}$  is defined to be 1 if an instance of a 3-node query motif or graph pattern exists between vertices  $(r, s, t)$  and 0 otherwise. More generally, we can define for any  $k$ -node query pattern a  $k$ -uniform hypergraph consisting of all instances of the query pattern in a given graph  $\mathcal{G}$ . Our algorithm will identify clusters of vertices in  $\mathcal{G}$  with a high number of pattern instances between them, which often have a functional meaning in biological networks [25, 27].

Another example for  $k = 3$  concerns the analysis and clustering of multiply linked data [28, 29]. Here we are given a set of  $M$  undirected graphs and define a hypergraph adjacency tensor as  $T_{ijm} = A_{ij}^{(m)}$ , where  $A^{(m)}$  denotes the adjacency matrix of the  $m^{\text{th}}$  graph. Clustering in this case identifies vertex sets which are densely connected in multiple, but not necessarily all, graphs.

## VII. ALGORITHM VALIDATION

The dominant eigenvector of a graph's adjacency matrix is often considered as a centrality measure ('eigenvector centrality' [1]) and is, in essence, equal to a simplified PageRank [30] for ranking global vertex importance.

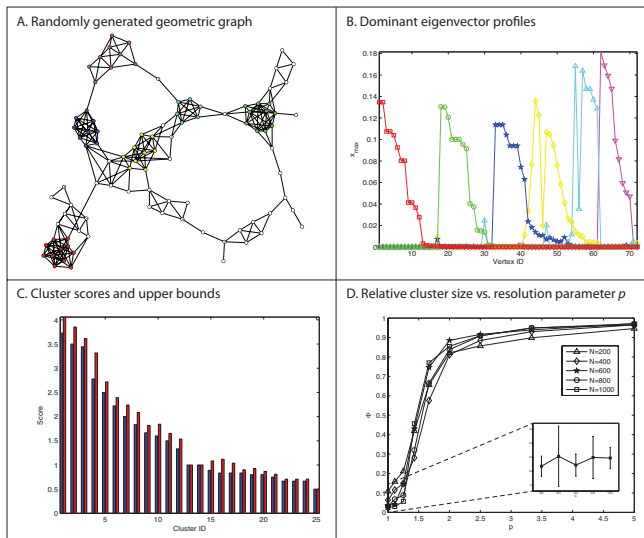


FIG. 1. **A.** Example of a randomly generated geometric graph with 100 vertices and radius 0.02, showing the largest connected component with the six highest-scoring edge clusters in color. **B.** Dominant eigenvector profiles for the six highest-scoring edge clusters with colors corresponding to panel A. **C.** Edge-to-node ratio scores (blue) and theoretical upper bound (red) for all 25 edge clusters. **D.** Triangle cluster size as the fraction  $\Phi$  of total number of network nodes for the highest-scoring cluster in random geometric graphs with  $N = 200, 400, 600, 800$  and  $1000$  nodes and constant edge density ( $\rho = 4$ ) as a function of  $p$ . Each data point is an average over 10 random networks. The insert shows the absolute mean cluster size and standard deviation over 10 random networks as a function of  $N$  for  $p = 1$ .

It may thus come as a surprise to see it playing a role in identifying localized clusters (however, see the references in the previous section). In order to demonstrate the validity of our approach, we applied it to randomly generated geometric graphs of various sizes (see Section X A for details), which are known to be a good model for biological interaction networks [31].

For visualization purposes, we generated as a toy example a random geometric graph with 100 vertices and radius  $r^2 = 0.02$  (Fig. 1A). The graph is evidently modular and the six highest-scoring edge clusters identified by our algorithm (with  $p = 1$ ) are indicated in color. The profiles of the corresponding dominant eigenvectors are clearly localized on a subset of nodes (Fig. 1B), illustrating that in a modular network, the dominant eigenvector indeed indicates the location of a single cluster, and should not be considered as a centrality measure. Furthermore, comparing the edge-to-node ratio for each of the discovered edge clusters with the theoretical upper bound in eq. (1) shows that the solution of the restricted variational problem (eq. (2)) must be close to the true maximum (Fig. 1C).

For a more systematic analysis we applied triangle-based clustering to sequences of geometric graphs with

constant expected edge density and varying size, i.e. define 3-uniform hypergraphs where each hyperedge corresponds to a triangle in the input graph. The parameter  $p$  can be used to identify clusters at different levels of resolution. Independent of network size, there is a low- $p$  phase where the fraction of nodes in a cluster is small compared to total network size, and a high- $p$  phase where a cluster consists of a macroscopic network portion (Fig. 1D). Interestingly, at  $p = 1$  (default edge-to-node ratio score), cluster size does not depend on network size (Fig. 1D, insert). Hence dominant eigenvector-based clustering does not suffer from a resolution limit problem where cluster size grows with network size irrespective of the presence of ‘natural’ clusters at smaller scales [32, 33]. As in the previous example, the cluster scores are always close to their theoretical upper bounds, demonstrating that the solution of the restricted variational problem is close to the true optimum in all cases (see Supp. Fig. S1).

## VIII. APPLICATIONS

### A. Tripartite community detection in online folksonomies

Folksonomies, online communities where users collaboratively create and annotate data, are examples of social systems that cannot be adequately modeled by ordinary graphs. For instance, tagged social networks such as Flickr [34] or CiteULike [35] have a tripartite structure that is best modeled by a 3-uniform hypergraph [5, 6]. Using CiteULike as a concrete example, each hyperedge consists of a user who has annotated an academic article with a certain keyword or tag [35] (Fig. 2A). Traditionally, the community structure of such tripartite networks has been analysed by applying standard community detection algorithms to one-mode ordinary graph projections of the hypergraph, *e.g.* by connecting two users if they have annotated the same articles or connecting two tags if they have been applied to the same articles [6]. In contrast, hypergraph-based clustering preserves the tripartite structure of folksonomy data and reveals additional levels of community structure. We applied our spectral clustering algorithm to a subset of the CiteULike dataset containing more than 400,000 (user, article, tag) entries and identified nearly 14,000 hyperedge clusters (see Section X B for details). The additional level of detail present in hyperedge clusters is illustrated by looking at the user, article or tag overlap between clusters. Fig. 2B shows an example of two hyperedge clusters formed by the same set of users who have annotated different sets of articles by different sets of tags. One tag, ‘pattern recognition’, is common between both clusters. The remaining tags show that the articles in the first cluster are about collective computing and swarm intelligence, whereas those in the second cluster deal with image analysis (Supp. Table S1), which are indeed two

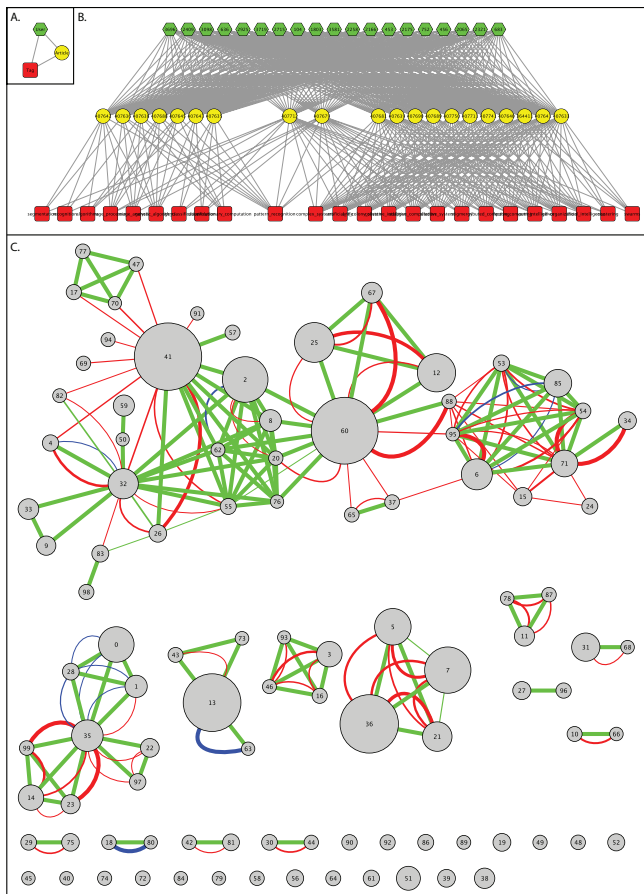


FIG. 2. **A.** CiteULike hyperedge which represents one instance of a user (green node) who has annotated an article (yellow node) with a certain tag (red node). **B.** Example of two tripartite communities where the same set of users (top) has annotated two sets of articles (middle) with two sets of tags (bottom). Only the two central articles and one central tag (‘pattern recognition’) overlap between the two clusters. User-tag edges have been omitted for clarity. **C.** Coarse-grained view of the CiteULike hypergraph using the 100 highest-scoring hyperedge clusters. Each node represents a cluster (node size proportional to number of hyperedges in the cluster) and edges represent significant overlap between clusters (overlap score  $> 0.5$ , edge size proportional to overlap score). Green edges, user overlap; red edges, tag overlap; blue edges, article overlap.

distinct subjects within the broad field of pattern recognition.

In general, we expect such sub-divisions of one-dimensional communities to occur at the level of users (*i.e.* the same set of users annotating different sets of articles using different sets of tags), but much less at the level of articles or tags (*i.e.* we do not expect different sets of users to annotate the same set of articles using different sets of tags, or to use the same set of tags for different sets of articles). Indeed, the 100 highest-scoring clusters (which together contain about 20% of all hyperedges) overlap predominantly at the user level, to a much

lesser extent at the tag level, and hardly at the article level, while about 21 of these clusters do not have any significant overlap (overlap  $> 50\%$ , see Section X B for details) with any other cluster (Fig. 2C). Significant article overlap occurs in only two instances. In both cases, it concerns a subset of users who have annotated a subset of articles from a larger cluster with an additional set of tags. Tag overlap occurs more frequently than article overlap, but with lower overlap percentages than user overlaps. Overlapping tags are typically general tags which can be applied to a broad spectrum of articles. For instance, the ten tags occurring most frequently in the top 100 clusters are: bibtex-import, learning, social, evolution, review, support, govt, non-us, collaboration, design. Thus we conclude that hyperedge clusters capture topic-specific tripartite (user, article, tag) communities which reveal more structure of the underlying data than user, article or tag communities based on a single data-dimension only.

## B. Local and global alignment of complex networks

The core idea for applying hypergraph clustering to integrated multi-network analysis is to translate the relation between multiple complex networks into higher-order hypergraph edges. We illustrate this idea by showing that local and global alignment of complex networks with a bipartite many-to-many mapping between their vertex sets can be naturally viewed as a hypergraph clustering problem.

Network alignment is the problem of finding topologically similar regions between two or more networks. In local network alignment, small subgraphs in each network are aligned independent of the alignment of other subgraphs, whereas global network alignment aims to find a unique, maximal alignment for each connected component in the input graphs. Network alignment methods for comparing molecular interaction networks between different species come in two main flavors. Topological network alignment finds conserved regions between networks taking only the topology of each network into account [36]. The second class of methods takes into account that networks in different species have evolved from a common ancestor through gene duplication and divergence mechanisms and hence that there exists a meaningful mapping between the nodes in each network [9]. Methods have been developed which assume a one-to-one mapping [37], but in general a many-to-many map should be considered [38].

More formally, consider two simple graphs  $\mathcal{G}_1$  and  $\mathcal{G}_2$ , whose vertices are connected by a bipartite graph  $\mathcal{M}$ . The directed alignment hypergraph  $\mathcal{H}$  between  $\mathcal{G}_1$  and  $\mathcal{G}_2$  is defined as the 4-uniform hypergraph containing the edges  $(\{i, j\}, \{k, l\})$  if and only if  $\{i, j\} \in \mathcal{G}_1$ ,  $\{k, l\} \in \mathcal{G}_2$  and  $\{i, k\}, \{j, l\} \in \mathcal{M}$  (see Fig. 3A). In a local alignment, we search for compact regions in each graph which align nearly perfectly with each other, *i.e.*, have a high



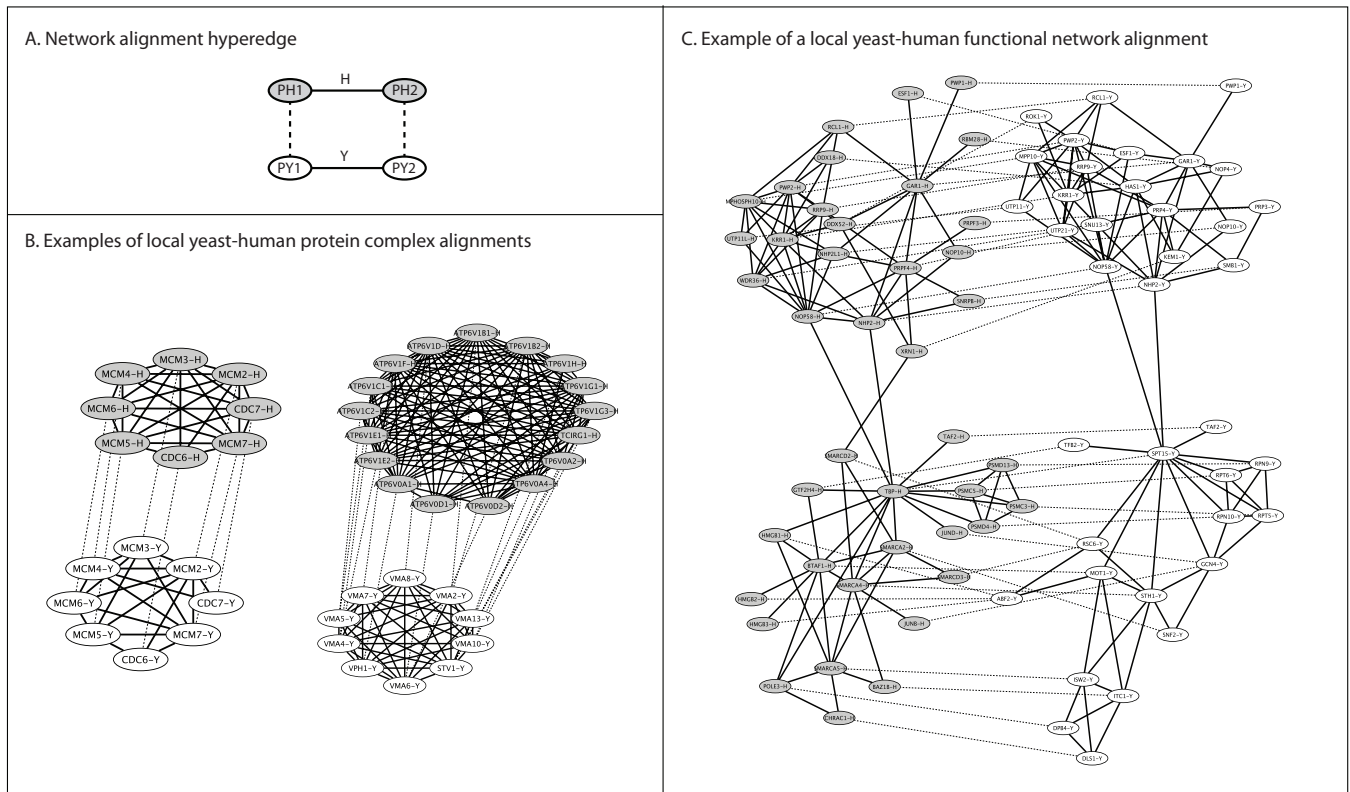


FIG. 3. **A.** A (directed) hyperedge in the yeast-human protein interaction network alignment hypergraph is a so-called *interolog*: a pair of interacting yeast (Y) proteins and a pair of interacting human (H) proteins connected by orthology relations (dashed lines). **B.** Examples of aligned protein complexes (clustering parameter  $p = 1$ , Cluster no. 19 left, no. 1 right). **C.** Example of a functional network alignment (clustering parameter  $p = 1$ , Cluster no. 48). In all panels, yeast proteins are white and human proteins are grey; protein interactions are solid and orthology relations are dashed.

density of alignment hyperedges between them. This corresponds to hypergraph clusters which maximize  $\mathcal{S}_p$  for values of  $p$  close to one. In a global alignment we search for maximally matching regions in each graph, *i.e.*, irreducible components in the alignment hypergraph. These correspond to hypergraph clusters which maximize  $\mathcal{S}_p$  for large values of  $p$ .

We used our hypergraph clustering algorithm to locally and globally align protein-protein interaction networks for yeast and human using orthology groups for mapping conserved proteins in each network (see Section X C for details). Typical examples of high-scoring local alignment clusters are conserved protein complexes (cf. Supp. Table. S2). Fig. 3B shows two examples: first a set of proteins which map one-to-one between yeast and human from the MCM complex, which plays an important role in DNA replication and is indeed conserved among all eukaryotes [39]; the second example is a set of components of the V-type ATPase (a proton pump) which has expanded in human compared to yeast by gene duplications [40]. Other local alignment clusters reflect more general functional networks than protein complexes (cf. Supp. Table S3). Fig. 3C shows an example of a conserved network involved in nucleic acid metabolism centred around

the general transcription factor, TBP (SPT15 in yeast), the TATA-binding protein. The largest irreducible component in the network alignment hypergraph (clustered with  $p = 10$ ) maps 651 yeast proteins to 766 human proteins and contains 90% of all interologs (Supp. Fig. S2 and Supp. Table S4), showing that there exists a high degree of network conservation at a global scale, consistent with previous findings using topological network alignment [36].

### C. Path clustering in regulatory networks

Unlike protein-protein interaction networks, which represent binary, undirected associations between proteins, regulatory networks, which control the cellular response to external or internal perturbations, are directed and represent the flow of information within a cell [7]. Standard community detection methods, which identify densely interconnected subsets of nodes, are therefore of limited use to analyze regulatory networks. In transcriptional regulatory networks, the response to perturbations can be measured experimentally by genetically knocking-out a transcription factor (TF) and measuring the result-

ing changes in gene expression levels on a genome-wide scale [41]. In yeast, direct physical binding interactions between a TF and its target genes [42] as well as perturbational response data for the same TF [41] are available for a comprehensive set of almost 200 TFs (see Section XD for details). On average only 3% of the perturbational targets are also direct physical targets of a TF. Understanding the mechanisms of indirect regulation and propagation of network perturbations has therefore been of considerable interest [43–46].

Hypergraph-based clustering presents a natural formalism for addressing this problem by considering each shortest path between two nodes in a network as a hyperedge in a non-uniform hypergraph. Clustering in this case identifies sets of nodes with a high number of shortest paths running through them and such clusters could potentially form ‘signal-propagation’ modules, consistent with the notion that at the single-node level, high information flow is associated to high values of a node’s betweenness, *i.e.*, the number of shortest paths passing through that node. To test this hypothesis, we calculated all directed shortest paths in the regulatory network of yeast between a TF and the genes differentially expressed upon knock-out of that TF. The resulting hypergraph contained 1332 hyperedges between 788 nodes and spectral clustering identified 25 non-singleton and 14 singleton clusters (see Materials and Methods for details). Topologically, there appear to exist two distinct types of path clusters. Combinatorial path clusters contain genes responding to the knock-out of multiple TFs and form a network of densely overlapping paths. Fig. 4A shows a combinatorial cluster of 199 shortest paths from 20 TFs to 186 genes involved in glycolysis and gluconeogenesis. Hierarchical path clusters on the other hand have a layered structure, where the perturbational signal of usually not more than one TF flows to its targets via a limited number of intermediate TFs, in a strictly hierarchical manner (Fig. 4B). The functional relevance of regulatory path clusters is demonstrated by the fact that they contain a significant fraction of the genes affected by the deletion of the cluster’s TF and that they are highly enriched for specific functional categories (cf. Supp. Tables S5 and S6). For simplicity, we considered here only shortest paths in the transcriptional regulatory network, but clearly the approach can be extended to paths composed of multiple interaction types.

## IX. CONCLUSIONS

Over the past decade, graph theory has become crucial to represent and reason about complex network data. In particular clustering, the detection of densely interconnected groups of vertices, has become a standard coarse-graining procedure to decompose complex networks into a limited number of presumably independently functioning units. With more and more data becoming available to highlight different aspects of the same complex sys-

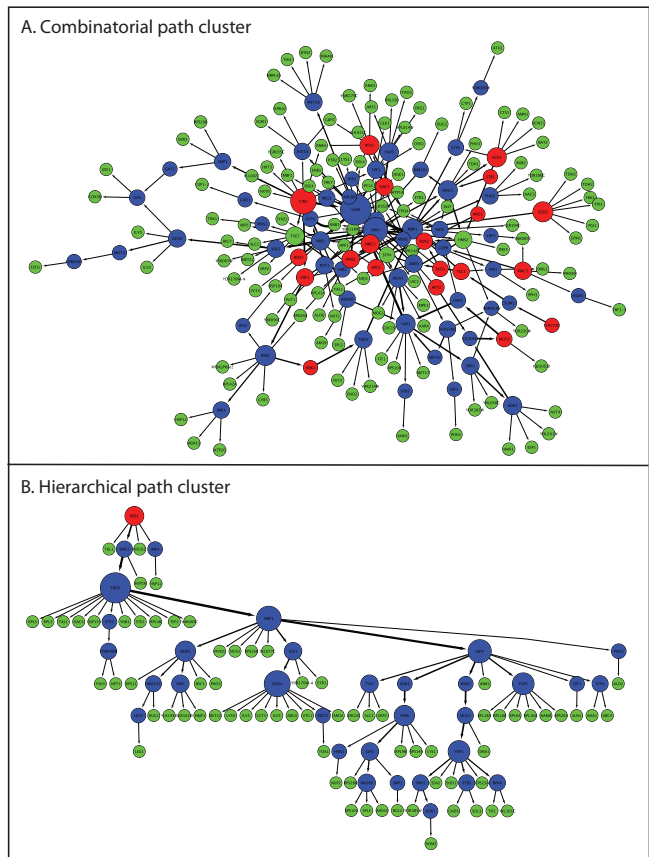


FIG. 4. Examples of a high-scoring combinatorial (A, Cluster no. 6) and hierarchical (B, Cluster no. 1) path clusters in the yeast transcriptional regulatory network. Red nodes, knocked-out transcription factors (TFs); green nodes, genes differentially expressed upon knock-out of the TFs; blue nodes, all other TFs. Node size, resp. edge width, is proportional to out-degree, resp. edge betweenness.

tems, a need has arisen to analyze networks with multiple types of interactions simultaneously. In this paper, we have proposed to use hypergraphs to characterize higher-order relations between simple graphs and we have introduced efficient algorithms for clustering and biclustering in such hypergraphs.

Our main result is a spectral clustering algorithm for hypergraphs, based on a generalization of the Perron-Frobenius theorem for directed and undirected hypergraphs. More precisely, we have shown that, like in ordinary graphs, there exists a unique, positive vector, called the dominant eigenvector, over the set of vertices of a hypergraph, which maximizes a natural generalization of the Rayleigh-Ritz ratio for matrices. The importance of this result lies in the fact that the ratio of the number of edges to the number of nodes in any subset of vertices can be expressed as the same Rayleigh-Ritz ratio, in graphs and hypergraphs alike. Densely interconnected clusters can therefore be found very efficiently by first computing the dominant eigenvector and then converting it to



a discrete set of vertices. Uniqueness of the dominant eigenvector guarantees unambiguity of the solution and rapid convergence of the numerical procedure, whereas positivity implies that the discretization can be achieved by setting an optimal threshold on its entries.

Our work has been motivated by concrete problems of data integration in social and biological networks. We have given three practical examples for using hypergraph-based clustering in these contexts, namely the detection of tripartite communities in folksonomies, the alignment of protein-protein interaction networks between multiple species using interolog clustering and the identification of common regulatory pathways in perturbational expression data using shortest path clustering. Undoubtedly, many more applications for hypergraph-based clustering exist in the analysis of other biological, social, computer, communication or neural networks. From a theoretical point of view, we have considered the edge-to-node ratio as a simple quality score for clusters in graphs and hypergraphs. Although this score has many attractive properties, such as its direct relation with the dominant eigenvector and the absence of any resolution limit problems, it will still be of interest to generalize clustering algorithms based on other quality scores from graphs to hypergraphs as well. Popular methods like those based on minimal cutsets or modularity maximization also rely on spectral properties of, respectively, the graph Laplacian and modularity matrix. Although certain mathematical aspects, such as eigenvalue multiplicity and its implications on algorithm convergence and cluster discretization, are more complicated in these cases, we believe our work lays the theoretical foundations for future studies in this direction.

## X. NETWORK DATA AND NUMERICAL SETTINGS

### A. Geometric random graphs

A geometric graph with  $N$  vertices and radius  $r$  is defined by a set  $\mathcal{V}$  of points in a metric space and edges  $\mathcal{E} = \{(u, v) \in \mathcal{V} : 0 < \|u - v\| < r\}$ . We generated random geometric graphs by sampling with uniform probability  $N$  points in the unit square  $[0, 1] \times [0, 1]$  and taking the standard 2-norm as the distance measure. For a given vertex, the probability that it is connected to any other vertex is  $\pi r^2$ . Hence if we increase  $N$  while keeping  $\rho = Nr^2$  constant we obtain a sequence of random geometric graphs with constant average expected degree.

### B. Tripartite community detection in the CiteULike data

We obtained the complete ‘who-posted-what’ data from CiteULike [35] (<http://www.citeulike.org/faq/data.adp>), containing (as of Feb. 1st, 2012) 16,553,642

(user, article, tag) entries. To create a more manageable dataset, we considered all entries from 2005, resulting in a hypergraph of 466,948 (user, article, tag) hyperedges between 4,693 users, 121,071 articles and 36,489 tags. Recursive hypergraph spectral clustering with  $p = 1$  identified 13,987 clusters with at least two hyperedges; 4,616 hyperedges formed singleton clusters. To measure the user, article and tag overlap of two hyperedge clusters, we used the overlap score defined for two sets  $X$  and  $Y$  as

$$\text{ovlp}(X, Y) = \frac{|X \cap Y|}{\min(|X|, |Y|)}.$$

### C. Alignment of yeast and human PPI networks

We obtained physical protein-protein interactions (PPI) for yeast from the BioGRID [47] database and physical and functional PPIs for human from the BioGRID and STRING [48] databases. The yeast network had 36,391 interactions between 4,847 proteins; the human network 40,630 interactions between 9,602 proteins. We integrated these networks with orthology mappings from the InParanoid database [49]. There were 3,390 orthology relations between 2,245 yeast and 3,255 human proteins which had at least one interaction in their respective PPI networks. We performed recursive spectral clustering on the directed alignment hypergraph consisting of 2,567 interolog-hyperedges (cf. Fig. 3A). At  $p = q = 1$ , 180 clusters with at least two hyperedges were found; 119 hyperedges had no connections in the hypergraph, forming singleton clusters. The functional enrichment analysis of the local and global alignment clusters is given in Supp. Tables S2 and S3).

### D. Path clustering in the yeast transcriptional regulatory network

We obtained a network of 11,373 transcription factor (TF) binding interactions between 198 TFs and 3,535 target genes in yeast from [42] and knock-out microarray data for 266 TFs from [41]; 182 TFs with binding data also had knock-out data for a total of 7,090 perturbational interactions. We constructed a directed hypergraph consisting of 1,332 hyperedges and 788 nodes, where each hyperedge is a shortest path in the regulatory network between a TF and a gene differentially expressed upon knock-out of that TF. We defined the source set of a hyperedge as the knocked-out TF and the target set as the remainder of the path. Recursive spectral clustering identified 39 clusters of which 14 were singletons.

## E. Supplementary data and algorithm implementation

Input data and clustering results are available as flat text files from <http://omics.frias.uni-freiburg.de/supplementary-data>. An implementation of the clustering algorithm in the Java programming language is available from <http://omics.frias.uni-freiburg.de/software>.

## ACKNOWLEDGMENTS

TM thanks the Department of Mathematics of the University of California, Davis for warm hospitality during visits when part of this work was performed. The work of BN was supported in part by the National Science Foundation under grant DMS-1009502.

- 
- [1] M. E. J. Newman, *SIAM Review*, **45**, 167 (2003).
- [2] R. Albert and A.-L. Barabási, *Rev Mod Phys*, **74**, 47 (2002).
- [3] R. Milo, S. Shen-Orr, S. Itzkovitz, N. Kashtan, D. Chklovskii, and U. Alon, *Science*, **298**, 824 (2002).
- [4] M. E. J. Newman, *PNAS*, **103**, 8577 (2006).
- [5] G. Ghoshal, V. Zlatić, G. Caldarelli, and M. Newman, *Physical Review E*, **79**, 066118 (2009).
- [6] V. Zlatić, G. Ghoshal, and G. Caldarelli, *Physical Review E*, **80**, 036118 (2009).
- [7] U. Alon, *An introduction to systems biology: design principles of biological circuits* (Chapman & Hall/CRC, 2007).
- [8] X. Zhu, M. Gerstein, and M. Snyder, *Genes & Dev*, **21**, 1010 (2007).
- [9] R. Sharan and T. Ideker, *Nat Biotech*, **24**, 427 (2006).
- [10] D. Zhou, J. Huang, and B. Schölkopf, in *Advances in Neural Information Processing Systems (NIPS) 19*, edited by B. Schölkopf, J. C. Platt, and T. Hofmann (MIT Press, 2007) pp. 1601 – 1608.
- [11] A. Vazquez, *Physical Review E*, **77**, 066106 (2008).
- [12] S. Klamt, U.-U. Haus, and F. Theis, *PLoS Comp Biol*, **5**, e1000385 (2009).
- [13] A. Vazquez, *Journal of Statistical Mechanics: Theory and Experiment*, **2009**, P07006 (2009).
- [14] S. Fortunato, *Phys Rep*, **486**, 75 (2010).
- [15] M. Porter, J.-P. Onnela, and P. J. Mucha, *Notices of the AMS*, **56**, 1082 (2009).
- [16] R. A. Horn and C. R. Johnson, *Matrix analysis* (Cambridge University Press, 1985).
- [17] M. E. J. Newman, *Phys Rev E*, **74**, 036104 (2006).
- [18] G. H. Golub and C. F. Van Loan, *Matrix computations*, 3rd ed. (The Johns Hopkins University Press, 1996).
- [19] L. De Lathauwer, B. De Moor, and J. Vandewalle, *SIAM J Matrix Anal Appl*, **21**, 1324 (2000).
- [20] K. Inoue and K. Urahama, *Pattern Recogn Lett*, **20** (1999).
- [21] J. M. Kleinberg, *J ACM*, **46**, 604 (1999).
- [22] L.-H. Lim, in *Proceedings of the IEEE International Workshop on Computational Advances in Multi-Sensor Adaptive Processing* (2005) pp. 129–132.
- [23] K. C. Chang, K. Pearson, and T. Zhang, *Commun Math Sci*, **6**, 507 (2008).
- [24] S. Friedland, S. Gaubert, and L. Han, *Lin Alg Appl* (2011), doi:10.1016/j.laa.2011.02.042.
- [25] T. Michoel, A. Joshi, B. Nachtergaele, and Y. Van de Peer, *Molecular BioSystems*, **7**, 2769 (2011).
- [26] P. Audenaert, T. Van Parys, M. Pickavet, P. Demeester, Y. Van de Peer, and T. Michoel, *Bioinformatics*, **27**, 1587 (2011).
- [27] L. V. Zhang, O. D. King, S. L. Wong, D. S. Goldberg, A. H. Y. Tong, G. Lesage, B. Andrews, H. Bussey, C. Boone, and F. P. Roth, *J Biol*, **4**, 6 (2005).
- [28] D. M. Dunlavy, T. G. Kolda, and W. P. Kegelmeyer, *Multilinear algebra for analyzing data with multiple linkages*, Tech. Rep. SAND2006-2079 (Sandia National Laboratories, Albuquerque, NM and Livermore, CA, 2006).
- [29] W. Li, C.-C. Lie, T. Zhang, H. Li, M. S. Waterman, and X. J. Zhou, *PLoS Comp Biol*, **7**, e1001106 (2011).
- [30] S. Brin and L. Page, *Computer Networks*, **30**, 107 (1998).
- [31] N. Pržulj, D. G. Corneil, and I. Jurisica, *Bioinformatics*, **20**, 3508 (2004).
- [32] S. Fortunato and M. Barthélemy, *PNAS*, **104**, 36 (2007).
- [33] B. H. Good, Y.-A. de Montjoye, and A. Clauset, *Phys Rev E*, **81**, 046106 (2010).
- [34] “Flickr,” <http://www.flickr.com>.
- [35] “CiteULike,” <http://www.citeulike.org>.
- [36] O. Kuchaiev, T. Milenkovic, V. Memisevic, W. Hayes, and N. Pržulj, *J R Soc Interface*, **7**, 1341 (2010).
- [37] J. Berg and M. Lässig, *PNAS*, **103**, 10967 (2006).
- [38] R. Sharan, S. Suthram, R. M. Kelley, T. Kuhn, S. McCuine, P. Uetz, T. Sittler, R. M. Karp, and T. Ideker, *PNAS*, **102**, 1974 (2004).
- [39] B. K. Tye, *Annu Rev Biochem*, **68**, 649 (1999).
- [40] H. Kibak, L. Taiz, T. S. P. Bernasconi, and J. P. Gogarten, *J Bioenerg Biomemb*, **24**, 415 (1992).
- [41] Z. Hu, P. Killion, and V. Iyer, *Nat Genet*, **39**, 683 (2007).
- [42] C. T. Harbison, D. B. Gordon, T. I. Lee, N. J. Rinaldi, K. D. Macisaac, T. W. Danford, N. M. Hannett, J. B. Tagne, D. B. Reynolds, J. Yoo, E. G. Jennings, J. Zeitlinger, D. K. Pokholok, M. Kellis, P. A. Rolfe, K. T. Takusagawa, E. S. Lander, D. K. Gifford, E. Fraenkel, and R. A. Young, *Nature*, **431**, 99 (2004).
- [43] T. Ideker, O. Ozier, B. Schwikowski, and A. F. Siegel, *Bioinformatics*, **18**, S233 (2002).
- [44] C. Workman, H. Mak, S. McCuine, J. Tagne, M. Agarwal, O. Ozier, T. Begley, L. Samson, and T. Ideker, *Science*, **312**, 1054 (2006).
- [45] A. Gitter, Z. Siegfried, M. Klutstein, O. Fornes, B. Oliva, I. Simon, and Z. Bar-Joseph, *Molecular systems biology*, **5** (2009).
- [46] A. Joshi, T. Van Parys, Y. Van de Peer, and T. Michoel, *Genome Biology*, **11**, R32 (2010).
- [47] C. Stark, B.-J. Breitkreutz, T. Reguly, L. Boucher, A. Breitkreutz, and M. Tyers, *Nucl Acids Res*, **34**, D535

(2006).

- [48] L. Jensen, M. Kuhn, M. Stark, S. Chaffron, C. Creevey, J. Muller, T. Doerks, P. Julien, A. Roth, M. Simonovic, *et al.*, *Nucleic acids research*, **37**, D412 (2009).
- [49] A. C. Berglund, E. Sjolund, G. Ostlund, and E. L. L. Sonnhammer, *Nucleic Acids Res*, **36**, D263 (2008).